JCI The Journal of Clinical Investigation

PD-1 blockade partially recovers dysfunctional virus–specific B cells in chronic hepatitis B infection

Loghman Salimzadeh, … , Patrick T.F. Kennedy, Antonio Bertoletti

J Clin Invest. 2018;128(10):4573-4587. https://doi.org/10.1172/JCI121957.

Research Article **Hepatology** **Infectious disease**

Chronic HBV (CHB) infection suppresses virus-specific T cells, but its impact on humoral immunity has been poorly analyzed. Here, we developed a dual-staining method that utilizes hepatitis B virus (HBV) surface antigens (HBsAg) labeled with fluorochromes as “baits” for specific ex vivo detection of HBsAg-specific B cells and analysis of their quantity, function, and phenotype. We studied healthy vaccinated subjects (n = 18) and patients with resolved (n = 21), acute (n = 11), or chronic (n = 96) HBV infection and observed that frequencies of circulating HBsAg-specific B cells were independent of HBV infection status. In contrast, the presence of serum HBsAg affected function and phenotype of HBsAg-specific B cells that were unable to mature in vitro into Ab-secreting cells and displayed an increased expression of markers linked to hyperactivation ($CD21^{lo}$) and exhaustion (PD-1). Importantly, B cell alterations were not limited to HBsAg-specific B cells, but affected the global B cell population. HBsAg-specific B cell maturation could be partially restored by a method involving the combination of the cytokines IL-2 and IL-21 and CD40L-expressing feeder cells and was further boosted by the addition of anti–PD-1 Abs. In conclusion, HBV infection has a marked impact on global and HBV-specific humoral immunity, yet HBsAg-specific B cells are amenable to a partial rescue by B cell–maturing cytokines and PD-1 blockade.

PD-1 blockade partially recovers dysfunctional virus–specific B cells in chronic hepatitis B infection

Loghman Salimzadeh,[1,2,3] Nina Le Bert,[1] Charles-A. Dutertre,[1,2] Upkar S. Gill,[4] Evan W. Newell,[2] Christian Frey,[5] Magdeleine Hung,[5] Nikolai Novikov,[5] Simon Fletcher,[5] Patrick T.F. Kennedy,[4] and Antonio Bertoletti[1,2]

[1]Emerging Infectious Diseases Program, Duke-NUS Medical School, Singapore. [2]Singapore Immunology Network, Singapore Agency for Science, Technology and Research (A*STAR), Singapore. [3]Department of Microbiology and Immunology, National University of Singapore, Singapore. [4]Barts Liver Centre, Barts and The London School of Medicine and Dentistry, Queen Mary University of London, London, United Kingdom. [5]Gilead Sciences Inc., Department of Biology, Foster City, California, USA.

Chronic HBV (CHB) infection suppresses virus-specific T cells, but its impact on humoral immunity has been poorly analyzed. Here, we developed a dual-staining method that utilizes hepatitis B virus (HBV) surface antigens (HBsAg) labeled with fluorochromes as "baits" for specific ex vivo detection of HBsAg-specific B cells and analysis of their quantity, function, and phenotype. We studied healthy vaccinated subjects (n = 18) and patients with resolved (n = 21), acute (n = 11), or chronic (n = 96) HBV infection and observed that frequencies of circulating HBsAg-specific B cells were independent of HBV infection status. In contrast, the presence of serum HBsAg affected function and phenotype of HBsAg-specific B cells that were unable to mature in vitro into Ab-secreting cells and displayed an increased expression of markers linked to hyperactivation ($CD21^{lo}$) and exhaustion (PD-1). Importantly, B cell alterations were not limited to HBsAg-specific B cells, but affected the global B cell population. HBsAg-specific B cell maturation could be partially restored by a method involving the combination of the cytokines IL-2 and IL-21 and CD40L-expressing feeder cells and was further boosted by the addition of anti–PD-1 Abs. In conclusion, HBV infection has a marked impact on global and HBV-specific humoral immunity, yet HBsAg-specific B cells are amenable to a partial rescue by B cell–maturing cytokines and PD-1 blockade.

Introduction

The coordinated activation of different components of the immune system is crucial for protection from pathogens. While innate immunity controls the initial response to infection, specific humoral and cellular immunity are required to eliminate the pathogen and prevent reinfection. The progressive functional inactivation of adaptive immunity characterizes persistent infections with alterations in both global and antigen-specific T and B cell compartments (1–5).

A similar situation is evident during hepatitis B virus (HBV) infection in which virus control is associated with the presence of functional antiviral T cells and with the serological detection of anti–HBV surface (anti-HBs) Abs (6). However, while the quantity and function of HBV-specific T cells have been clearly defined in chronic HBV (CHB) patients (7–12), detailed characterization of the anti-HBV–specific B cell response is lacking. In order to fill this knowledge gap, we developed a system that utilizes recombinant HBV surface antigens (HBsAg) labeled with 2 different fluorochromes for ex vivo detection of HBsAg-specific B cells by flow cytometry. This method is independent of the secretory function of Abs and allows precise measurement of the frequency and function of HBsAg-specific B cells.

Studies in CHB patients have reported activation (13) and reduced functional capacity (14) of the global B cell population and have typically been unable to detect anti-HBs–secreting B cells (15–17), which have been suggested as being deleted by HBsAg-specific $CD8^+$ T cells (18). However, the presence of HBsAg/anti-HBs immune complexes in the sera of CHB patients (19) and detection of rare anti-HBs Abs–producing cells in ELISpot assays performed on peripheral blood mononuclear cells (PBMCs) of CHB patients (14, 20) suggest that deletion or functional inactivation of HBsAg-specific B cells is not complete (21). The current study focused on HBsAg-specific B cells because, even though humoral responses target all HBV proteins (19), only anti-HBs–specific Abs are associated with the concept of functional HBV cure (serological negativity of HBV DNA and HBsAg) and protection (22, 23). Anti-HBs Abs target different epitopes located in the small surface protein of HBV (24) and exhibit a protective role by blocking the interaction of HBV with heparan sulfate molecules (25), but additional mechanisms, such as direct suppression of HBV production from infected hepatocytes (26, 27), have been suggested.

▶ Related Commentary: p. 4257

Authorship note: LS and NLB contributed equally to this work.
Conflict of interest: AB receives research support from Gilead Sciences Inc. to test the effect of HBV antigens on immune cell function. He acted as a consultant for and served on the advisory boards of Gilead Sciences Inc., MedImmune, Janssen-Cilag, Abivax, and HUMABS. He is also a cofounder of Lion TCR, a biotech company developing T cell receptors for treatment of virus-related cancers. PTFK has collaborative grant funding from Gilead Sciences Inc., participates on the advisory board of and provides consultancy to Gilead Sciences Inc. and Janssen-Cilag, and is an investigator for industry-led trials with Gilead Sciences Inc., Janssen-Cilag, Alere, and Assembly Biosciences. CF, MH, NN, and SF are employed by Gilead Sciences Inc.
Submitted: April 30, 2018; **Accepted:** July 26, 2018.
Reference information: *J Clin Invest*. 2018;128(10):4573–4587.
https://doi.org/10.1172/JCI121957.

Table 1. Details of the cohorts of chronic, acute, and resolved HBV patients and healthy vaccinated and unvaccinated subjects from this study

Clinical phases of HBV infection		Number of subjects	Age (yr)	HBsAg (log IU/ml)	HBV DNA (log IU/ml)	ALT (IU/l)
Chronic	HBeAg$^+$ chronic infection (immune tolerant)	22	23 ± 6	4.6 ± 0.45	8.5 ± 0.77	29.7 ± 11.8
	HBeAg$^+$ chronic hepatitis (immune reactive)	24	25 ± 4.7	3.9 ± 1.3	6.3 ± 2.5	65.6 ± 38.6
	HBeAg$^-$ chronic hepatitis (immune reactive)	24	27 ± 2.5	3.6 ± 0.6	4.5 ± 1.4	68.8 ± 81.2
	HBeAg$^-$ chronic infection (inactive carrier)	26	24 ± 4.2	3.5 ± 0.76	2.2 ± 0.7	28.9 ± 19.6
Acute		11 (6 subjects longitudinal)	33 ± 9.5	Positive	Positive	1865 ± 1141
Resolved (anti-HBs$^+$, anti-HBc IgG$^+$, HBsAg$^-$)		21	?	Negative	Negative	ND
Healthy vaccinated		18	31.6 ± 4.2	Negative	Negative	ND
Healthy unvaccinated		5	45.8 ± 20.3	Negative	Negative	ND

ND, not determined.

An unusual feature of the HBV replication cycle is that virus-infected hepatocytes secrete a large quantity of subviral particles (HBsAg) in addition to infectious virions. These noninfectious subviral particles vastly outnumber HBV virions in the circulation of CHB patients (by 10^3- to 10^6-fold) and can reach concentrations as high as 50 to 100 μg/ml (24). Importantly, the small S HBV protein is present in both viral and subviral particles, and thus, anti-HBs Abs target both HBV virions and HBsAg. The evolutionary reason that HBV has developed its ability to produce large quantities of subviral, noninfectious particles is still not clear. One attractive hypothesis is that HBsAg functions as a decoy to saturate anti-HBs Abs and so prevents virus neutralization (28). It has also been proposed that HBsAg can suppress innate, humoral, or cellular immunity (29). In this study, we developed a method to directly detect HBsAg-specific B cells ex vivo, which allows us to analyze the impact that HBsAg has on the quantity, phenotype, and function of virus-specific B cells and on potential strategies that can boost their functionality.

Results

Direct ex vivo detection of HBsAg-specific B cells. Direct visualization of HBsAg-specific B cells utilizing HBsAg-conjugated microbeads has been performed in HBsAg-vaccinated individuals (30), but not in patients with HBV infection in whom anti–HBV-specific B cells have so far been evaluated using functional assays that might underestimate their size (15–17). In order to detect low-frequency antigen-specific B cells (31), 2 batches of HBsAg (genotype A) were chemically labeled with 2 distinct fluorochromes, DyLight 550 and DyLight 650 (Figure 1A). The fluorochrome-labeled HBsAg reagents were designed to act as "bait" to bind specifically to anti-HBsAg B cell receptors (BCRs) on the cell surface of CD19$^+$ B cells.

To test this strategy, we evaluated peripheral blood samples from a healthy subject who received an HBV vaccine boost. Serum levels of IgG anti-HBs following the booster vaccination increased by day 7 and remained high until day 60 (Figure 1B). In addition, the frequency of total plasmablasts in the peripheral blood of this vaccinated subject reached maximum levels on day 7 after vaccination (Figure 1C), confirming that the booster vaccination worked successfully. We stained PBMCs isolated from this subject with DyLight 550– and DyLight 650–labeled HBsAg (HBsAg-D550 and HBsAg-D650) and Abs that allowed gating on total memory B cells (MBCs) (Supplemental Figure 1; supplemental material available online with this article; https://doi.org/10.1172/JCI121957DS1). Figure 1, D and E, shows the frequency of double-positive HBsAg-D550$^+$D650$^+$ MBCs (naive CD21$^+$CD27$^-$ excluded) within the total CD19$^+$ B cell population from the day of boost (day 0) to day 60 after HBV vaccination.

In parallel with the kinetics of total plasmablasts and Ab production, the frequency of double-positive HBsAg-D550$^+$/650$^+$ MBCs peaked at day 7, reaching 0.4% of total CD19$^+$ B cells (Figure 1E), and then gradually declined. This HBsAg double-positive B cell population principally comprised CD27^{hi}CD38^{hi} plasmablasts at day 7 to 9 after vaccination, while HBsAg-D550$^+$/650$^+$ plasmablasts were not detectable 15 days after booster vaccination (Figure 1D). Interestingly, the mean fluorescence intensity (MFI) of HBsAg-D550$^+$/650$^+$ double-positive B cells increased progressively over time (Figure 1F), as expected from MBCs that express higher levels of surface BCR than plasmablasts. Finally, no changes in the frequency of HBsAg-D550$^+$/650$^+$ B cells were detected on naive (CD21$^+$CD27$^-$) B cells (Supplemental Figure 1). These data suggest that our fluorochrome-conjugated HBsAg is able to directly detect ex vivo HBsAg-specific B cells.

To confirm this, HBsAg-D550$^+$/650$^+$ and HBsAg-D550$^-$/650$^-$ MBCs were sorted and cultured in vitro after polyclonal stimulation to induce expansion, plasmablast differentiation, and Ab production. Only HBsAg-D550$^+$/650$^+$ B cells secreted anti-HBs Abs, as measured by ELISA and ELISpot assays (Figure 1G). Thus, HBsAg-D550 and HBsAg-D650 can identify HBsAg-specific B cells directly ex vivo at a single-cell level.

Frequency of HBsAg-specific B cells during HBV infection. We first utilized HBsAg-D550 and HBsAg-D650 to measure the frequency of HBsAg-specific B cells in the peripheral blood of HBV-vaccinated subjects and patients acutely or chronically infected with HBV. The clinical and virological profiles of the tested subjects are summarized in Table 1. We studied 18 healthy vaccinated subjects, 11 acute (HBsAg$^+$, IgM anti-core$^+$, high ALT), and 21 resolved (anti-

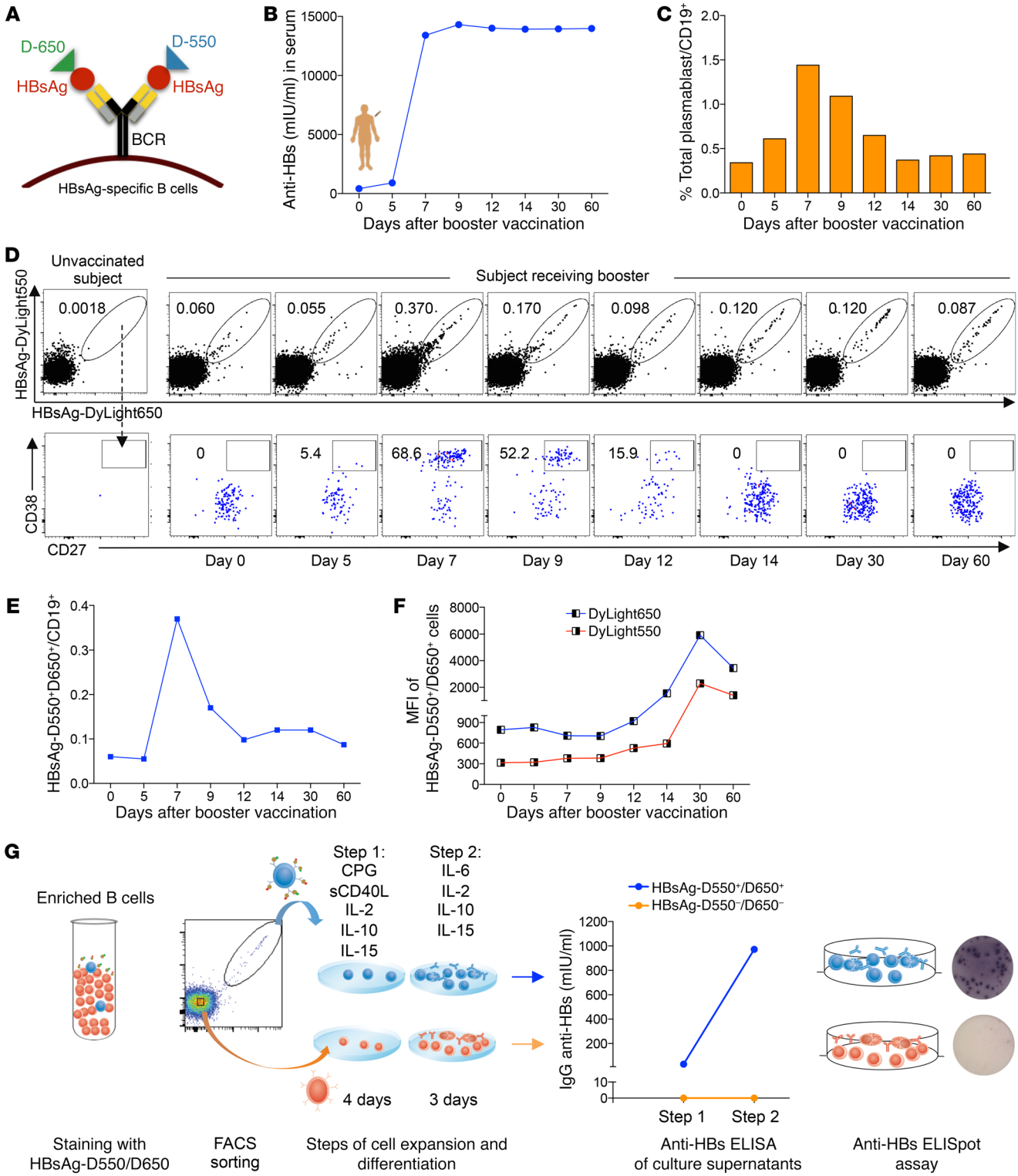

Figure 1. Fluorescently labeled HBsAg baits bind specifically to HBsAg-specific B cells. (**A**) Schematic representation of fluorescently labeled HBsAg baits binding to the BCR on the surface of HBsAg-specific B cells. A healthy subject received an HBV booster vaccination. Serum and blood samples were analyzed from day 0 to day 60 after vaccination. (**B**) Anti-HBs titers in the serum from day 0 to day 60 after vaccination. (**C**) Frequency of total plasmablasts ($CD19^+CD10^-CD21^{-/lo}CD27^{++}CD38^{++}$) out of total B cells measured longitudinally. (**D**) Flow cytometry plots show the frequency of HBsAg double-binding MBCs (top panel) and their percentages displaying a plasmablast phenotype (bottom panel). The first plot at the left shows data of a healthy unvaccinated subject. The other plots show data of a healthy vaccinated subject at the indicated time points before and after the HBV booster vaccination. (**E**) Frequency of HBsAg double-binding MBCs over time. (**F**) MFI of HBsAg-D550 and HBsAg-D650 on HBsAg-specific B cells at different time points. (**G**) Equal numbers of $HBsAg\text{-}D550^+D650^+$ and $HBsAg\text{-}D550^-D650^-$ MBCs were FACS sorted from PBMCs of day 60 after booster vaccination and triggered for Ab production by CpG and sCD40L polyclonal activation. Cells were cultured in 2 different steps with different cytokine mixtures. Subsequently, anti-HBs ELISA and anti-HBs ELISpot assays were performed on culture supernatants and on the cells, respectively.

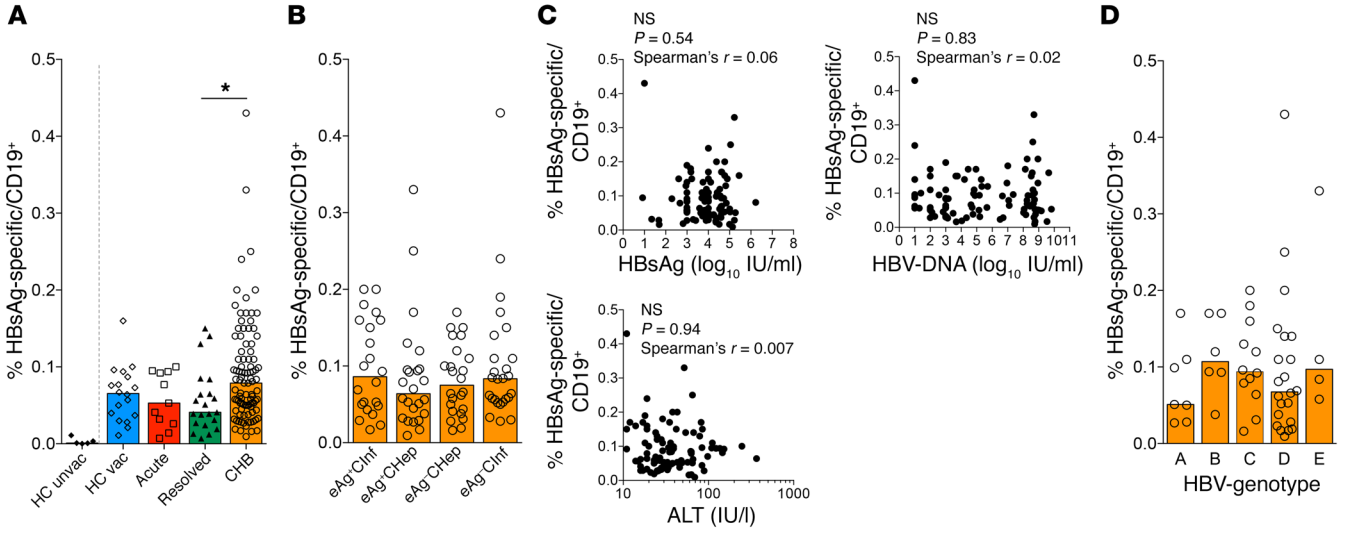

Figure 2. Similar frequency of HBsAg-specific B cells in diverse cohorts of HBV-infected patients. (**A**) Frequency of HBsAg-specific B cells in 5 healthy HBV-unvaccinated (HC unvac), 18 healthy HBV-vaccinated (HC vac), 11 acute HBV, 21 resolved HBV, and 96 CHB patients out of total CD19$^+$ B cells. (**B**) Frequency of HBsAg-specific B cells out of total CD19$^+$ B cells in different phases of CHB: 22 HBeAg$^+$ chronic infection (eAg$^+$CInf), 24 HBeAg$^+$ chronic hepatitis (eAg$^+$CHep), 24 HBeAg$^-$ chronic hepatitis (eAg$^-$CHep), and 26 HBeAg$^-$ chronic infection (eAg$^-$CInf). (**C**) No correlation between frequency of HBsAg-specific B cells and serum levels of HBsAg, HBV DNA, and ALT. (**D**) Frequency of HBsAg-specific B cells among 51 CHB patients infected with 5 different HBV genotypes. Data are presented as median, and statistical analysis was performed by the Kruskal-Wallis test followed by Dunn's multiple comparisons test. *$P < 0.05$ (**A**, **B**, and **D**); Spearman's rank correlation (**C**).

HBs$^+$ and anti–HBV core$^+$ [anti-HBc$^+$]) as well as 96 CHB patients (HBsAg$^+$) divided into the following clinical phases: 22 HBV e-antigen$^+$ (HBeAg$^+$) chronic infection, 24 HBeAg$^+$ chronic hepatitis, 24 HBeAg$^-$ chronic hepatitis, and 26 HBeAg$^-$ chronic infection (32). In addition, PBMCs of 5 healthy non–HBV-vaccinated subjects (anti-HBs and anti-HBc negative) were included as controls.

Figure 2A shows the frequency of HBsAg-specific B cells in the different cohorts. HBsAg-D550$^+$/650$^+$ B cells were detected at variable frequencies in all HBV-vaccinated subjects and HBV-infected patients tested. In contrast, they were not detected in 4 out of the 5 healthy nonvaccinated controls and were detected only at a very low frequency (0.01% of total B cells) in 1 of these controls, demonstrating the high specificity of the dual-staining detection method.

The median (interquartile range) frequency of HBsAg-specific B cells in the different cohorts was remarkably similar (vaccinated, 0.065% [0.035%–0.088%]; acute, 0.053% [0.026%–0.094%]; resolved, 0.041%[0.025%–0.074%); chronic, 0.079%[0.048%–0.12%]), even though it was slightly higher in patients with CHB versus those with resolved infection. There was large variability of HBsAg-specific B cell frequencies between different subjects with CHB, in whom HBsAg-specific B cells could be detected at levels ranging from to 0.01% to 0.43% of total B cells. However, these different frequencies were not associated with distinct clinical or virological profiles of HBV infection. Deconvolution of HBsAg-specific B cell frequency in different categories of CHB patients showed comparable variability in all phases of CHB (Figure 2B), with the median frequency (approximately 0.1% of total B cells) identical in all cohorts of CHB patients. There was also no statistically significant association between HBsAg-specific B cell frequency and serum levels of HBsAg, HBV DNA, and alanine aminotransferase (ALT) (Figure 2C).

We hypothesized that the marked variability of HBsAg-specific B cells detected in CHB patients may be related to the genotype of the infecting virus. Since our fluorochrome-conjugated HBsAg reagents are based on HBV genotype A, a possibility is that our reagents would preferentially bind B cells specific for HBsAg genotype A or D (which are genetically closely related), but not B cells specific for other genotypes (B, C, and E, which are more distant).

Accordingly, the HBV genotypes for 51 out of 96 CHB patients were determined. As shown in Figure 2D, a similar frequency of HBsAg-specific B cells was detected in CHB patients irrespective of the genotype of the infecting virus. Thus, the frequency of HBsAg-specific B cells is comparable in patients irrespective of their natural history stage. This contrasts with the features of HBV-specific T cells, which are present in higher frequencies in patients who resolve HBV than in those with CHB infection (33).

In order to further analyze the relationship between HBsAg-specific B cell frequency and viral control, we studied patients with acute hepatitis B infection from the time of onset of clinical symptoms to functional cure (i.e., HBV DNA negativity, HBsAg loss, and detection of anti-HBs).

First, we investigated whether the B cell compartment is activated during acute hepatitis B. We thus measured the frequency of plasmablasts (CD19$^+$, CD10$^-$, CD21$^-$, CD27^{hi}, CD38^{hi}) in 6 acute hepatitis B patients and, as controls, in 5 patients with acute dengue infection (Figure 3A). Frequency of plasmablasts was extremely low in 5 out of the 6 patients analyzed at all the different time points. A single subject showed a frequency of 6.5% of plasmablasts out of total B cells at the onset of acute hepatitis. In contrast, high frequency of plasmablasts was easily detected (16%–37% of total B cells) in 4 of the 5 acute dengue patients studied within a week of the onset of dengue symptoms. Their detection was transient, since 2 weeks after the acute phase, the plas-

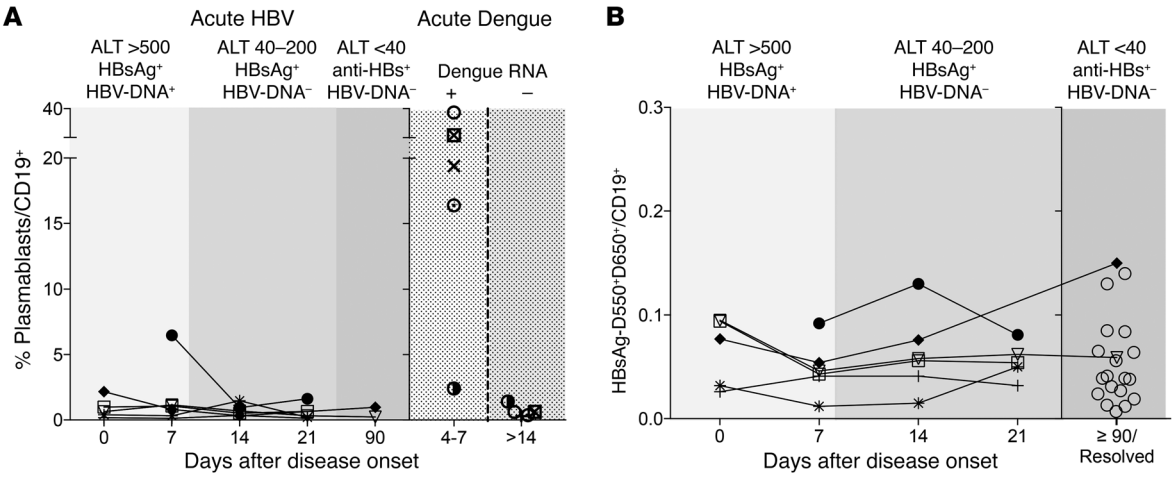

Figure 3. Longitudinal profile of B cell responses in acute HBV patients. (**A**) Frequency of global plasmablasts ($CD19^+CD10^-CD21^-CD27^{++}CD38^{++}$) out of total B cells ($CD19^+$) were analyzed at the indicated different time points in 6 patients with acute HBV (left) and in 5 patients with acute dengue infection (right). Time points are indicated as days after onset of clinical symptoms. Virological features of acute HBV and dengue are indicated at the top of the figures. (**B**) Longitudinal frequency of HBsAg-specific B cells in the 6 acute hepatitis B patients compared with the frequency obtained in 21 subjects with resolved HBV infection (anti-HBc^+, anti-HBs^+; open circles). HBsAg-specific B cells were calculated as the frequency of memory double-positive HBsAg-$D550^+D650^+$ B cells out of total $CD19^+$ B cells. Each symbol represents a single patient.

mablast frequency fell below 1.5% of total B cells. Thus, during the symptomatic phase of acute hepatitis B, the initiation of a B cell response is not detectable in the circulating compartment. In line with the lack of a robust B cell response, the frequency of HBsAg-specific B cells remained remarkably stable in all of the 6 acute HBV patients analyzed over time despite the changes in HBV DNA and ALT and the development of anti-HBs Ab (Figure 3B). HBsAg-specific B cell frequency during acute hepatitis B was similar to the frequency detected in resolved patients (anti-HBs^+ and anti-HBc^+ patients with a history of hepatitis). Thus, the B cell immunity profile appears remarkably stable during the acute symptomatic phase of acute hepatitis B, and the quantity of circulating HBsAg-specific B cells does not correlate with that of HBV control.

Function of HBsAg-specific B cells during HBV infection. The lack of correlation between HBsAg-specific B cell frequency and HBV control might indicate that HBsAg-specific B cells present in different groups of HBV-infected subjects have functional differences. Indications that anti-HBs–producing B cells are functionally altered in CHB infection have already been suggested by data derived from the analysis of bulk B cells (15–17).

To further decipher the functionality of HBsAg-specific B cells, we sorted HBsAg-specific B cells from 14 CHB patients and measured their ability to proliferate and mature into Ab-secreting B cells. HBsAg-specific B cells of healthy vaccinated individuals (4 subjects) were also sorted as controls. HBsAg-specific B cells of all 4 vaccinated individuals expanded in vitro and produced anti-HBs Abs (Figure 4A). However, microscopic inspection of the cell culture of HBsAg-specific B cells of CHB patients revealed that, in most of the cases, B cells expanded poorly or disappeared. ELISpot assays to analyze the frequency of HBV-specific B cells were performed in only 5 chronic patients, and anti-HBs Ab spots were detected in a single culture (Figure 4A). Parallel analysis of anti-HBs Ab titers in supernatants of all cultured HBAg-specific B cells of CHB patients confirmed that anti-HBs Abs were detected at very low titers only in 1 of the 14 HBsAg-specific B cell cultures tested (Figure 4B).

We reasoned that HBsAg-specific B cells present in CHB patients might require help from feeder cells to properly expand. We thus adopted a different protocol of B cell maturation that utilizes fibroblasts overexpressing CD40L as feeder cells and specific cytokines (IL-2 and IL-21) (34). Similar numbers of HBsAg-specific B cells were again sorted from 16 CHB patients and from 8 healthy controls, expanded for 13 days, and then analyzed for the presence of anti-HBs–secreting cells by ELISpot assay. Figure 4C shows that we were able to recover the ability of HBsAg-specific B cells to mature into anti-HBs–secreting B cells in 11 out of 16 tested CHB patients. With this method, the sorted cells survived and expanded well, but their maturation capacity was still compromised (mean spot counts: healthy = 240 spots, CHB = 22 spots). Taken together, these data directly demonstrate that functional impairment affects HBsAg-specific B cells of CHB patients in comparison with those present in healthy vaccinated individuals.

In addition, we analyzed the functionality of HBsAg-specific B cells present in acute hepatitis B patients. HBsAg-specific B cells were sorted at the indicated time points from PBMCs of 5 acute patients (Figure 5) and were expanded using the 2 protocols (with or without feeder cells) utilized to expand HBsAg-specific B cells of CHB patients. Note that the limited sample availability made it impossible to test the HBsAg-specific B cells from the same patient and time point with both protocols. Anti-HBs titers in the supernatants (Figure 5A) and quantity of anti–HBs-producing B cells (Figure 5B) were measured after 7 or 13 days of expansion. Surprisingly, HBsAg-specific B cells of acute HBV patients sorted during the acute phase of hepatitis B ($HBsAg^+$ phase), similarly to those of CHB patients, did not differentiate from Ab-secreting cells and did not produce Abs irrespective of their expansion method. In contrast, HBsAg-specific B cells sorted from PBMCs collected after HBsAg seroconversion in 3 out of the 3 tested patients

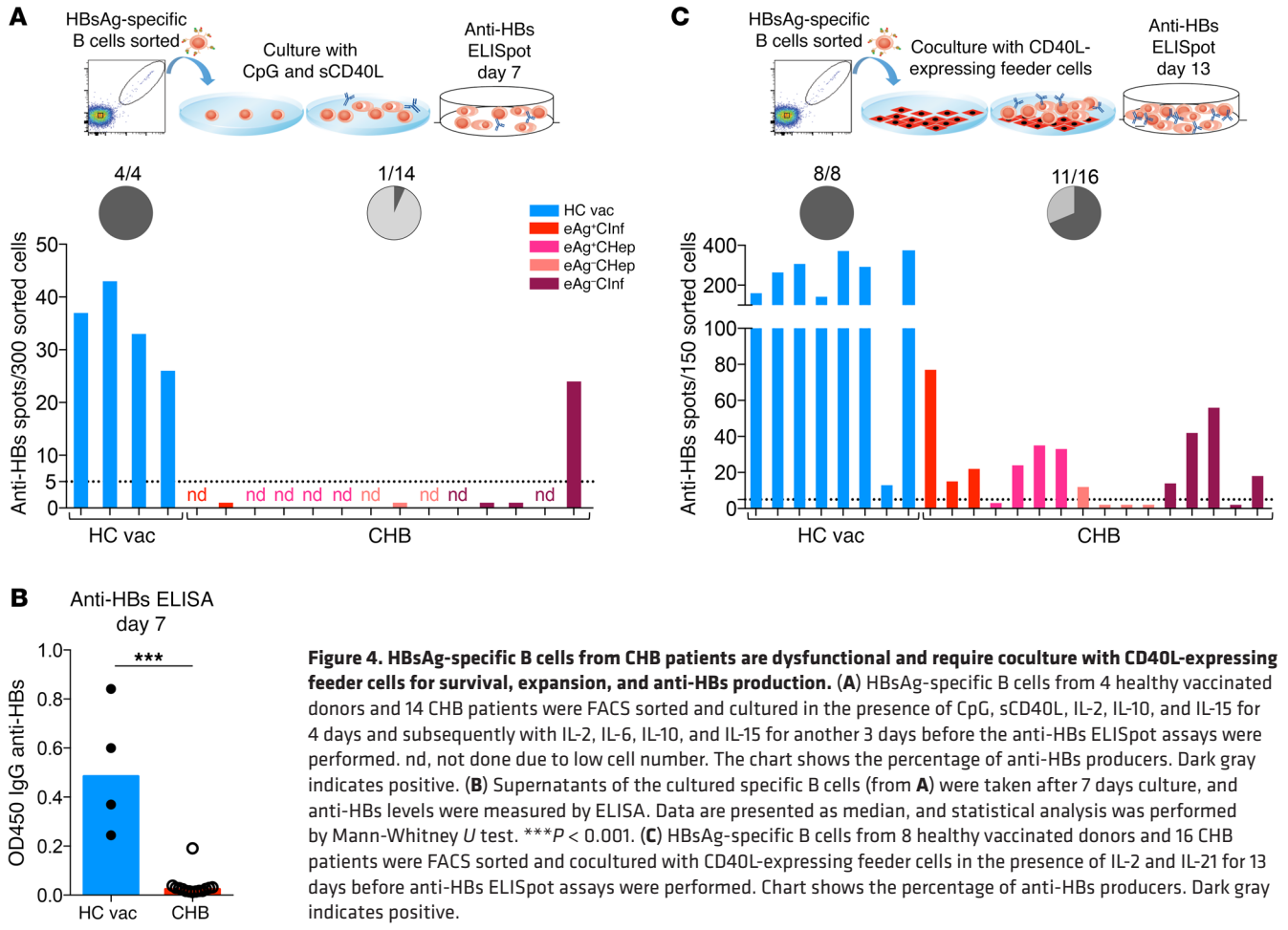

Figure 4. HBsAg-specific B cells from CHB patients are dysfunctional and require coculture with CD40L-expressing feeder cells for survival, expansion, and anti-HBs production. (**A**) HBsAg-specific B cells from 4 healthy vaccinated donors and 14 CHB patients were FACS sorted and cultured in the presence of CpG, sCD40L, IL-2, IL-10, and IL-15 for 4 days and subsequently with IL-2, IL-6, IL-10, and IL-15 for another 3 days before the anti-HBs ELISpot assays were performed. nd, not done due to low cell number. The chart shows the percentage of anti-HBs producers. Dark gray indicates positive. (**B**) Supernatants of the cultured specific B cells (from **A**) were taken after 7 days culture, and anti-HBs levels were measured by ELISA. Data are presented as median, and statistical analysis was performed by Mann-Whitney *U* test. ***$P < 0.001$. (**C**) HBsAg-specific B cells from 8 healthy vaccinated donors and 16 CHB patients were FACS sorted and cocultured with CD40L-expressing feeder cells in the presence of IL-2 and IL-21 for 13 days before anti-HBs ELISpot assays were performed. Chart shows the percentage of anti-HBs producers. Dark gray indicates positive.

expanded and produced anti-HBs (Figure 5, A and B). Thus, HBsAg-specific B cells present during acute HBV infection display functional impairment similar to those detected in CHB patients, but recover their functionality after HBsAg$^+$ seroconversion. Conjointly, the data obtained in chronic and acute HBV patients suggest that HBsAg modulates the functionality of HBsAg-specific B cells irrespective of the outcome of HBV infection.

Phenotype of B cells during HBV infection. To understand the possible causes of the impaired functionality of HBsAg-specific B cells, we analyzed and compared the phenotype of HBsAg-specific and total B cells present in patients with acute and chronic HBV as well as in those with resolved infection along with vaccinated subjects. In other chronic infections (e.g., HCV, HIV, and malaria), B cells, with reduced expression of the complement receptor type 2 (CD21) and of the memory marker CD27, are present in augmented frequencies. They are defined as atypical memory (AtM) B cells and show a reduced ability to proliferate and produce Abs after stimulation with B cell activators (3–5).

To characterize the phenotype of HBsAg-specific B cells, we performed analysis of flow cytometric data using the algorithm Uniform Manifold Approximation and Projection (UMAP). This algorithm enables visualization of high-dimensional cell parameters in a 2D map by plotting cells with similar phenotypes in close proximity (35). Live total MBCs (CD19$^+$CD10$^-$; CD21$^+$CD27$^-$ naive B cells excluded) and HBsAg-D550$^+$/650$^+$ MBCs from a total of 141 samples were concatenated and analyzed for the expression of markers that define MBC subsets (CD21, CD24, CD27, CD38, IgG) and their activation status (CD19, CD23, CD39, CD69, CD73, CD95, HLA-DR, PD-1). UMAP analysis automatically separated plasmablasts (CD24$^-$CD38^{hi}), classical IgG$^+$ and IgG$^-$ MBCs, and AtM B cells (CD21$^-$CD27$^-$) (Figure 6A).

Next, we analyzed the phenotypic profile of HBsAg-specific B cells from 15 healthy vaccinated and 76 CHB patients with different disease phases by overlaying them onto the concatenated UMAP of total MBCs (Figure 6B). This revealed that HBsAg-specific B cells generally have a heterogeneous phenotype; however, in CHB patients only, we detected an accumulation of HBsAg-specific cells within the cluster of AtM B cells. While only 5.5% of HBsAg-D550$^+$/650$^+$ B cells from healthy vaccinated subjects were present within the AtM cluster defined by UMAP, the number was 14.7% for CHB patients (Figure 6C).

Since UMAP did not separate the classical CD21$^+$CD27$^+$ resting memory (RM) and CD21$^-$CD27$^+$ activated memory (AM) MBC subsets and only allows comparison of samples stained with an identical Ab panel, we also quantified the phenotypic distribution of HBsAg-specific and total B cells using manual gating strategies (Supplemental Figure 2). This showed clearly that most HBsAg-specific B cells of healthy vaccinated and CHB patients displayed a phenotype of RM B cells and confirmed again that a significantly higher proportion of HBsAg-specific B cells of CHB patients dis-

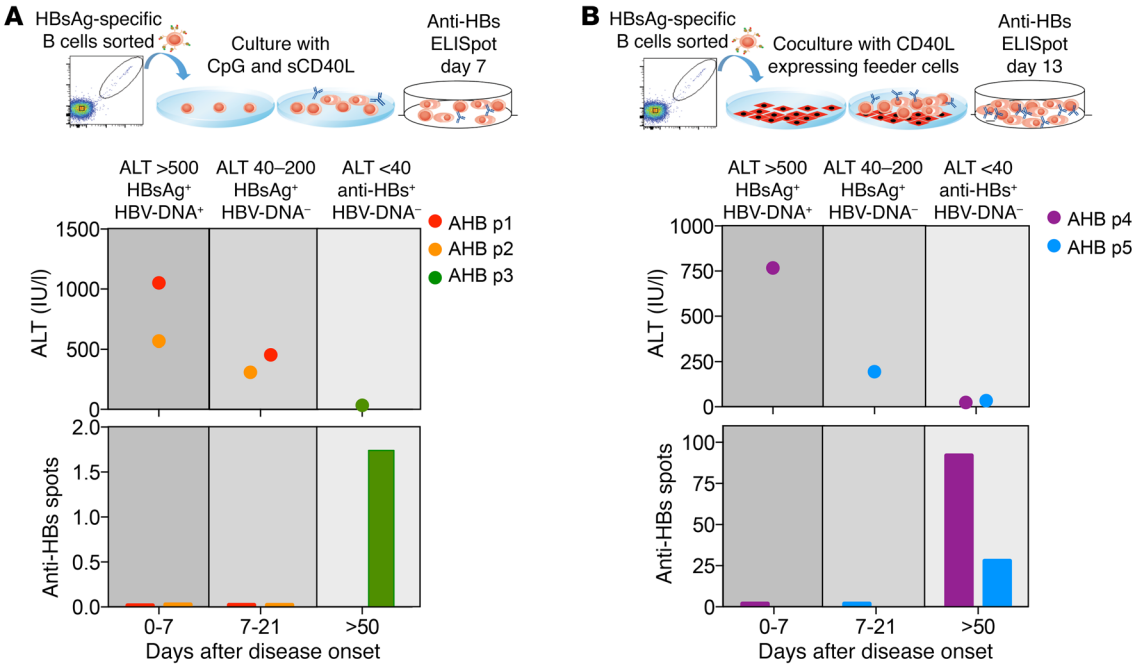

Figure 5. Functional characterization of HBsAg-specific B cells during acute hepatitis B. (**A**) HBsAg-specific B cells were sorted from PBMCs of 3 patients at different time points after onset of acute hepatitis B (AHB). The schematic graph on the top indicates the different serological and clinical parameters (ALT, HBsAg, and HBV DNA) at which PBMCs were collected. Sorted HBsAg-specific B cells were polyclonal stimulated with CpG, sCD40L, IL-2, IL-10, and IL-15 for 4 days and subsequently cultured with IL-2, IL-6, IL-10, and IL-15 for another 3 days. After 7 days, culture supernatants were collected and tested in an anti-HBs–specific ELISA. Bars indicate the optical density of detected anti-HBs Ab. (**B**) HBsAg-specific B cells were sorted from PBMCs of 2 additional acute hepatitis B patients at the indicated time points. Sorted HBsAg-specific B cells were expanded on CD40L-expressing fibroblasts with the addition of IL-2 and IL-21 for 13 days. Expanded cells were tested on anti-HBs B cell ELISpot. Bars indicate the numbers of spots obtained.

played an AtM phenotype (16.6% CHB, 8.4% HBV vaccinated; $P = 0.01$; Supplemental Figure 2).

The frequency of HBsAg-specific B cells with an AtM phenotype was identical in different cohorts of CHB patients (Figure 6C) and was not correlated with HBsAg quantity, HBV DNA, or ALT (Supplemental Figure 3). Importantly, the modification of the B cell phenotype was not selectively present in the HBsAg-specific B cell compartment, but an enriched frequency of AtM was also detected in total B cells, which declined with progressing phases of CHB infection (Figure 6D). In line with this decline, we found a positive correlation between HBV DNA values and frequency of global AtM B cells, but not with serum HBsAg levels (Figure 6E).

In addition, we analyzed to determine whether HBsAg-specific B cells present during the HBsAg$^+$ serological phase of acute hepatitis were associated with a preferential AtM phenotype (Figure 6, F and G). Despite the significant decline of HBV DNA, ALT, and HBsAg values during the course of acute hepatitis B, we failed to detect any consistent pattern in terms of AtM phenotype frequency of HBsAg-specific B cells at different time points during acute hepatitis (Figure 6G). One patient had a very high frequency (67%) of HBsAg-specific B cells with an AtM phenotype at the onset of acute HBV infection, and in this patient, the HBsAg-specific B cells with an AtM phenotype decreased sharply over time (Figure 6G). Yet the overall frequency of AtM in HBsAg-specific B cells of patients with acute HBV infection was not statistically different from that in resolved or vaccinated subjects (Figure 6F). However, the global B cell compartment of acute HBV patients was significantly enriched for AtM in comparison with that of healthy vaccinated subjects (Figure 6H). Again, we found no consistent pattern of global AtM frequency during acute hepatitis B (Figure 6I).

Alteration of the global B cell compartment during HBV infection. The increased frequency of total B cells with an AtM phenotype supports the notion that HBV infection might influence, not only the HBV-specific, but also the global B cell compartment. Evidence of the impact of HBV infection on total B cells has been previously reported (13, 36). We analyzed the transcriptional profile of the 4 different mature B cell subsets of healthy vaccinated and CHB patients with high viral replication and absence of inflammation (HBeAg$^+$ chronic infection). CD19$^+$CD10$^-$ B cells were sorted based on their expression of CD21 and CD27 (Figure 7A). In parallel, naive and memory populations of CD4$^+$ and CD8$^+$ T cells, using anti-CCR7 and anti-CD45RA, were also sorted to determine whether differential gene expression is more pronounced on the B or T cell compartment (Figure 7B). First, to better understand the properties of AtM B cells present in CHB patients, we compared their gene expression profile to those of classical MBCs, RM, and AM (Supplemental Figure 4). This revealed that they are similar to AtM B cells found enriched in patients with persistent HIV, HCV, and *Plasmodium falciparum* infection, characterized by upregulation of, e.g., *TBX21*, *FCRL5*, *FCRL3*, *LILRB2*, and *SIGLEC6* and downregulation of *CCR7*, *SELL*, and *IL13RA* (3, 4, 37–39). Moreover, after sorting the different global MBC subsets, we confirmed that AtM B cells enriched in CHB patients were similarly defective

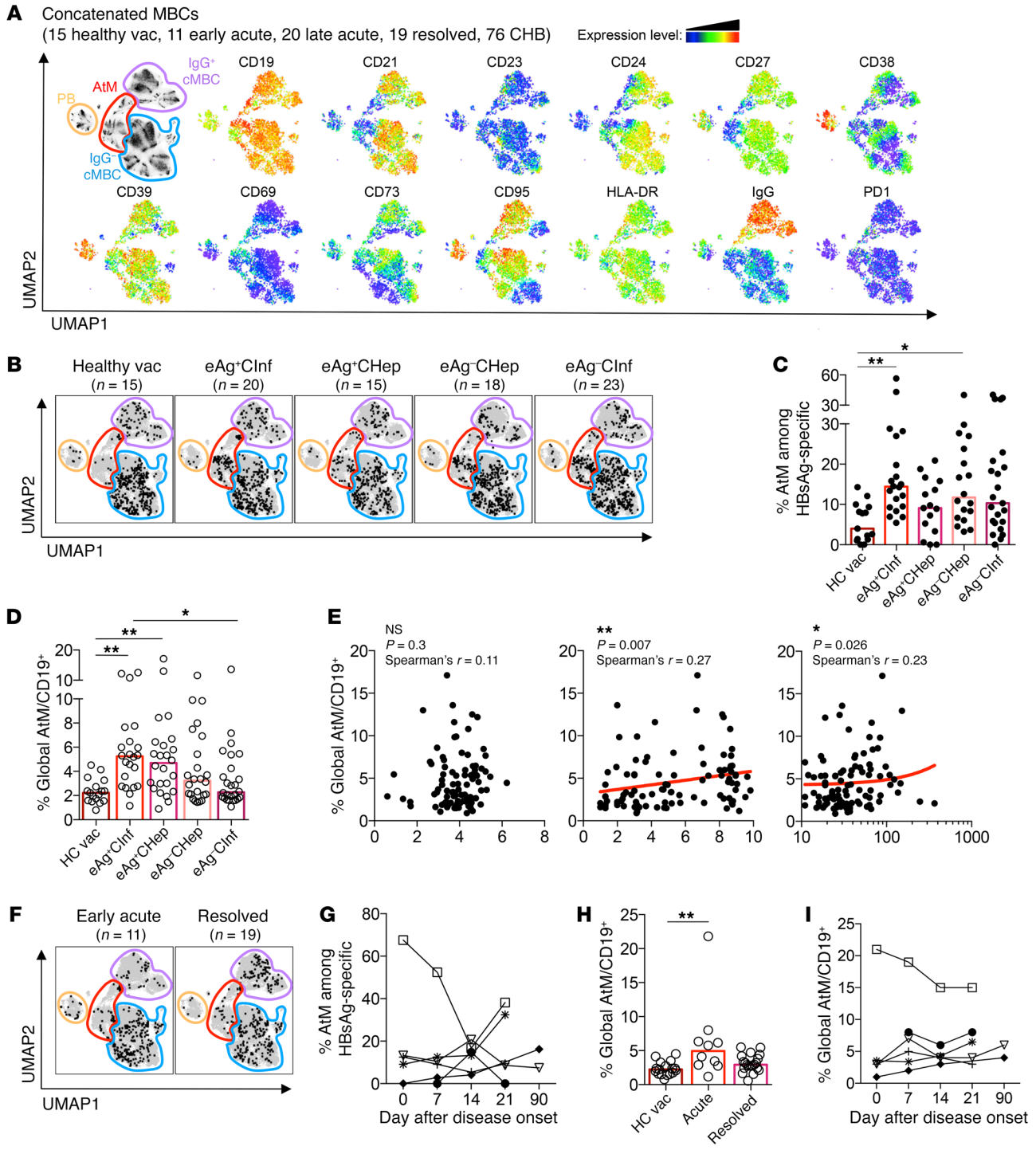

Figure 6. HBsAg-specific and global B cells of CHB patients are enriched for an AtM phenotype. (**A**) Flow cytometric data of MBCs from 15 healthy vaccinated, 11 early acute, 20 late acute, 19 resolved, and 76 CHB patients were analyzed by the dimensionality reduction algorithm UMAP and concatenated. Four different MBC subsets were delineated (left panel) based on the expression heatmaps of 13 markers (right panels). (**B**) HBsAg-specific B cells from 15 healthy vaccinated, 20 HBeAg$^+$ chronic infection, 15 HBeAg$^+$ chronic hepatitis, 18 HBeAg$^-$ chronic hepatitis, and 23 HBeAg$^-$ chronic infection patients were concatenated, normalized to their correct frequency, and overlaid onto the UMAP plot of global concatenated MBCs. (**C**) Frequency of AtM B cells among HBsAg-specific B cells within the different cohorts. (**D**) Frequency of global AtM B cells among total B cells (CD19$^+$) present in the subjects of the different cohorts. (**E**) Correlation of frequency of global AtM among total B cells with serum HBsAg (left), HBV DNA (middle), and ALT (right) levels. (**F**) Overlay of HBsAg-specific B cells on global MBCs of 11 concatenated acute (left) and 19 resolved (right) HBV patients. (**G**) Percentage of HBsAg-specific B cells with an AtM phenotype in 6 acute HBV patients at different time points from disease onset. Each symbol represents a single patient. (**H**) Percentage of global AtM B cells among total B cells (CD19$^+$) of healthy vaccinated, acute, and resolved HBV patients. (**I**) Percentage of global AtM B cells in 6 acute HBV patients at different time points from disease onset. Bar graphs present median, and statistical analysis was performed by the Kruskal-Wallis test followed by Dunn's multiple comparisons test (**C**, **D**, and **H**) and Spearman's rank correlation (**E**). *$P < 0.05$; **$P < 0.01$.

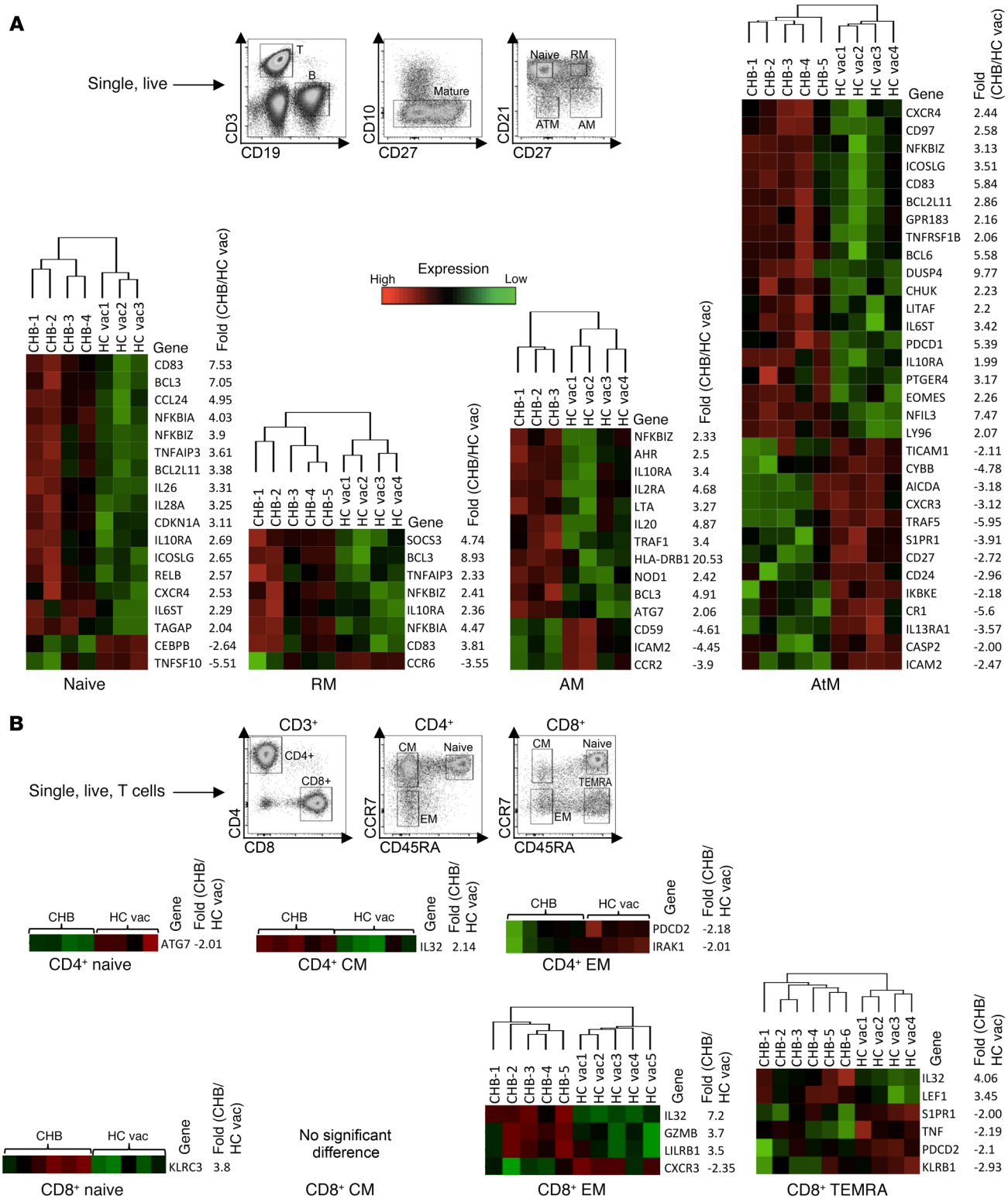

Figure 7. Transcriptional alteration of global B cell subsets by CHB infection. (**A**) Four different mature ($CD19^+CD10^-$) B cell populations from 5 CHB patients (CHB; eAg^+CInf) and 4 healthy vaccinated subjects were FACS sorted based on their expression of CD21 and CD27 (see gating strategy). Cells were lysed, and mRNA expression levels of 588 immune-related genes were measured by NanoString. Heatmaps showing immune genes that are significantly different between CHB and healthy vaccinated subjects ($P < 0.05$, ≥2-fold different) within the 4 different B cell subsets, naive, RM, AM, and AtM. (**B**) Four different subsets of global $CD4^+$ and $CD8^+$ T cells ($CD3^+$) were sorted from 6 CHB patients and 5 healthy vaccinated controls based on their expression of CCR7 and CD45RA (see gating strategy) and analyzed by NanoString. EM, effector memory; CM, central memory. Heatmaps showing immune genes that are significantly different between CHB and healthy vaccinated subjects ($P < 0.05$, ≥2-fold different) within the different T cell subsets.

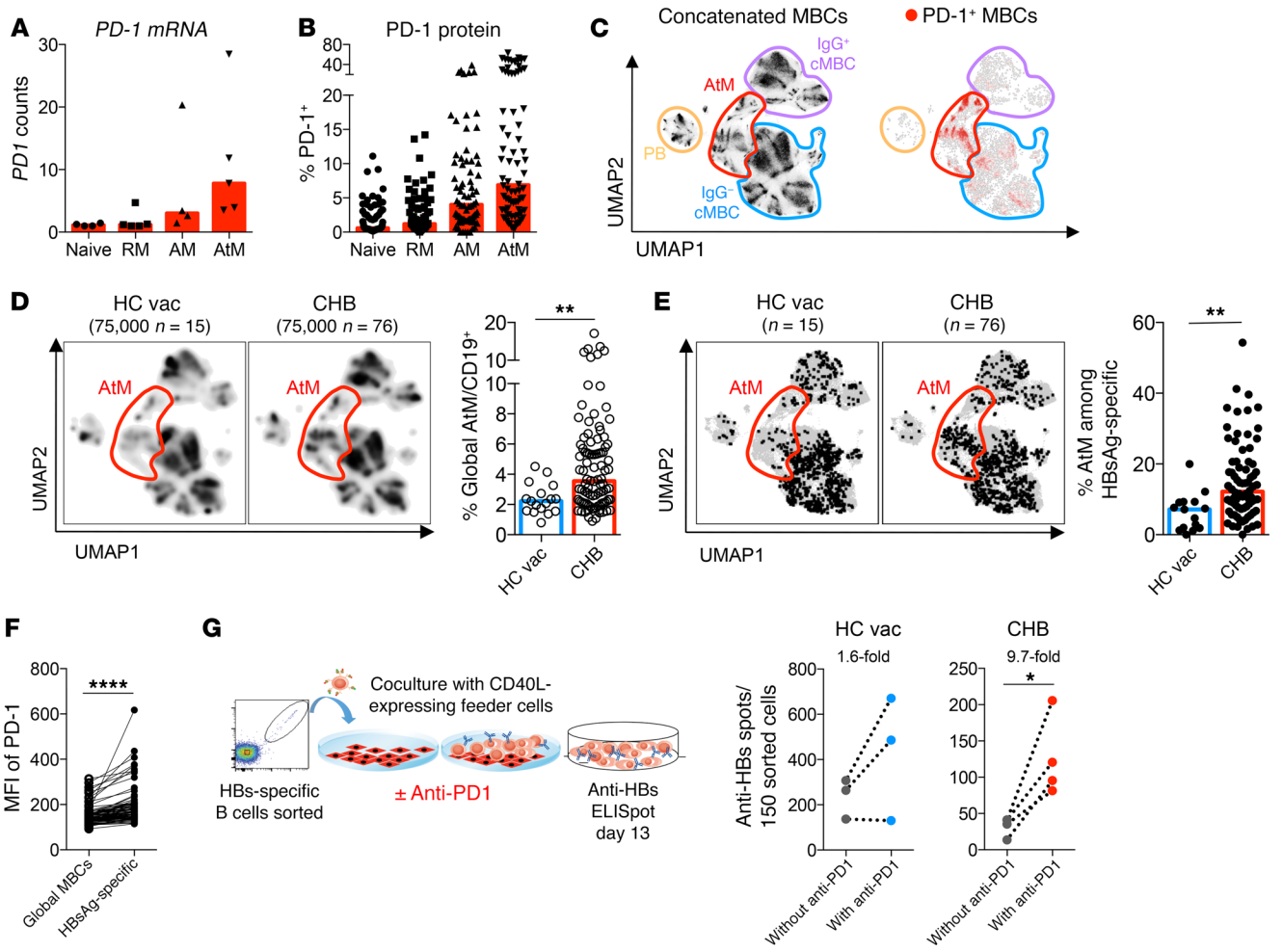

Figure 8. PD-1 blockage partially recovers dysfunctional HBsAg-specific B cells of CHB patients. (**A**) mRNA expression of *PD-1* in the indicated B cell subsets of 5 CHB patients measured by NanoString. (**B**) Surface PD-1 expression on the B cell subsets of 96 CHB patients measured by flow cytometry. (**C**) Flow cytometric data of MBCs from 141 samples analyzed by UMAP and concatenated. Four subsets of MBCs were delineated (left, plots reshown from Figure 6A), and PD-1$^+$ MBCs are shown (right). (**D**) MBCs of 15 healthy vaccinated (left) and 76 CHB patients (right) were downsampled to equal cell numbers. Density UMAP plots are shown; the cluster of AtM B cells is highlighted in red. Right bar graph shows percentage of global MBCs with an AtM phenotype in 17 healthy vaccinated and 96 CHB patients. (**E**) Double-positive HBsAg-D550$^+$D650$^+$ B cells from 15 healthy vaccinated (left) and 76 CHB patients (right) were concatenated, downsampled to normalized frequencies, and overlaid onto the UMAP plot of global concatenated MBCs; the cluster of AtM B cells is highlighted in red. Right bar graph shows percentage of HBsAg-specific B cells with an AtM phenotype in healthy vaccinated and CHB patients. (**F**) MFI of PD-1 on global MBCs and HBsAg-specific MBCs of 96 CHB patients. (**G**) Double-positive HBsAg-D550$^+$D650$^+$ MBCs from 4 CHB patients and 3 healthy vaccinated subjects were FACS sorted and cocultured for 13 days with CD40L-expressing feeder cells in the presence of IL-2 and IL-21, with or without anti–PD-1 Ab (schematic at left). Subsequently, anti-HBs–secreting cells were detected by ELISpot assay (right). Average fold changes in the number of anti-HBs spots are shown above the plots. Data are presented as median, and statistical analysis was performed by the Mann-Whitney *U* test (**D** and **E**) and Wilcoxon's paired *t* test (**F** and **G**). **P* < 0.05; ***P* < 0.01; *****P* < 0.0001.

in expansion and differentiation into Ab-secreting cells (total IgG) upon polyclonal CpG activation (Supplemental Figure 4B).

Then we analyzed to determine whether the 4 B cell subsets (naive, RM, AM, and AtM) of healthy and CHB patients display differences in their gene expression profile. In all the 4 B cell subsets combined, a total of 55 genes were differentially regulated (>2-fold different, $P < 0.05$; total of 588 immune genes measured), but the AtM B cells were the more diversified by HBV infection, with 32 genes differentially regulated. Strikingly, the gene expression profiles of naive and memory CD4$^+$ and CD8$^+$ T cells of CHB patients and healthy controls were more homogeneous, with only 12 genes differentially regulated in the 7 T cell populations compared.

Among the most upregulated genes in B cells of CHB patients were some related to B cell activation, such as CD83, a costimulatory molecule induced on B cells by activated T cells through CD40 engagement (40). CD83 was upregulated on naive, RM, and AtM B cells of CHB patients. Also, all 4 B cell populations present in CHB patients upregulated NFKBIZ, which is induced following BCR or TLR stimulation (41). We also noted differential expression of genes involved in B cell differentiation. DUSP4, a tumor-suppressor gene in B cell lymphoma, was upregulated by 9.8-fold in AtM of CHB patients compared with healthy controls. It has a role in inhibiting cell proliferation and differentiation through the inhibition of MAPK. We also observed that *ICAM-2* was downregulated

on AM and AtM B cells ($CD21^{lo}$ B cells) of CHB patients. ICAM-2 is essential for long-lasting cognate T follicular helper (Tfh)/B cell interactions and efficient selection of low-affinity B cell clones for proliferative clonal expansion (42). Importantly, we detected an increased expression of PD-1 within AtM B cells of CHB-infected patients. A hallmark of CHB infection is the presence of exhausted HBV-specific T cells (8), but whether HBV infection can affect the global B and T cell populations remains controversial. In the 5 CHB patients studied here, unlike what occurs in AtM B cells, the activation inhibitor PD-1 was not overexpressed in any of the tested T cell subsets of CHB patients.

Collectively, these data show that HBV infection appears to exert a more pronounced impact on the global B cell than T cell population and that functional modulation is not restricted to HBsAg-specific B cells, but is also seen in the global B cell compartment.

Rescue of HBsAg-specific B cell function with anti–PD-1 Abs. Increased mRNA expression of *PD-1* in AtM B cells of CHB patients led us to hypothesize that PD-1 blockade can further boost HBsAg-specific B cell differentiation into Ab-secreting cells. PD-1 is a negative regulator of T cell activation, but it is also expressed by B cells and can regulate human B cell maturation (43). Importantly, siRNA downregulation of PD-1 expression recovers the HIV-specific exhausted B cell response (44), and anti–PD-1 treatment of SIV-infected macaques boosts functionality of antiviral T and B cells (45).

We determined that mRNA and protein expression of PD-1 were elevated on AM and specifically AtM B cells compared with the classical RM B cells (Figure 8, A–C). In addition, the global AtM B cell population was enriched by HBV infection (Figure 8D) and was also enriched in HBsAg-specific B cells of chronically infected patients (Figure 8E). Since HBsAg-specific B cells express higher levels of PD-1 compared with global MBCs (Figure 8F), we tested in vitro whether PD-1 blockade can affect the Ab-secreting cell maturation of HBsAg-specific B cells present in CHB patients.

Sorted HBsAg-specific B cells of 4 CHB patients (3 $HBeAg^+$ infection, 1 $HBeAg^+$ hepatitis) and 3 healthy vaccinated subjects were cultured with CD40L-expressing fibroblasts with or without anti–PD-1 Ab. Figure 8G shows that anti–PD-1 treatment was able to increase the number of anti-HBs–producing B cells preferentially in the CHB patients tested. The ability to mature into Ab-secreting cells increased on average by 9.7-fold in the CHB patients and by 1.6-fold in healthy vaccinated subjects. Although the number of Ab-producing cells was still lower in CHB patients, our data demonstrate that PD-1 blockade can partially restore the anti-HBs secretory ability of HBsAg-specific B cells.

Discussion

We performed here a comprehensive ex vivo analysis of the frequency, function, and phenotype of HBsAg-specific B cells in patients with different profiles of HBV infection. This study allows us to begin to define the features of humoral immunity against HBV, which has previously been largely neglected.

The first observation is that the quantity of circulating HBsAg-specific B cells is remarkably similar in vaccinated subjects and in patients with acute or chronic HBV infection. We did not find any associations between the frequency of HBsAg-specific B cells and HBsAg or HBV DNA quantity in chronic infection. Furthermore, the numbers of circulating HBsAg-specific B cells are stable during the symptomatic phase of acute HBV infection despite the robust changes in HBV DNA and HBsAg levels characteristic of acute hepatitis B.

These findings differ from circulating HBV-specific T cell frequency, which is inversely proportional to the level of HBV DNA in adult patients with CHB infection (33) and fluctuates vigorously during acute hepatitis B (46). At first sight, this discrepancy could be interpreted as a sign that B cells have a limited role in controlling HBV, but the ability of HBV-specific MBCs to suppress HBV is indirectly supported by data from rituximab-treated subjects (47, 48). CD20-expressing B cell depletion treatment is known to trigger HBV reactivation in a high proportion of anti-HBc^+ subjects, and the importance of HBsAg-specific B cells during HBV infection is confirmed by our functional data. Indeed, the second clear observation of our work is that, while the frequency of circulating HBsAg-specific B cells is independent of the stage of HBV infection, their function is influenced by the presence of HBV infection itself and in particular by the presence or absence of serum HBsAg.

HBsAg-specific B cells of vaccinated individuals and of HBV-infected patients that have resolved HBV infection (anti-HBs^+ and anti-HBc^+) efficiently mature in vitro with different expansion/differentiation protocols. In contrast, HBsAg-specific B cells sorted from both chronic and acute (still in the $HBsAg^+$ phase) HBV-infected patients demonstrate clear functional defects. First, they were substantially unable to expand without the presence of feeder cells expressing CD40L. Furthermore, even though HBsAg-specific B cells were not completely exhausted and could be recovered in some CHB patients, their ability to expand and/or differentiate in the presence of CD40L interaction and cytokines (IL-2 and IL-21) remains defective in comparison with HBsAg-specific B cells present in HBsAg-negative subjects. These data confirm the historical work performed with bulk B cells that has indicated specific functional defects of HBsAg-specific B cells in CHB patients (15–17).

However, our demonstration that HBsAg-specific B cells of CHB patients can be partially rescued in vitro suggests that a residual functionality of HBsAg-specific B cells could be maintained in vivo in the presence of T helper and Tfh cells or in the proper anatomical location (lymph node) (49). This could explain why anti-HBs Abs can still be measured in the form of immunocomplexes in CHB patients (19).

At the moment, the causes of the partial functional defects of HBsAg-specific B cells are not entirely clear. HBsAg-specific B cells are likely to directly interact with the circulating HBsAg via their specific BCRs, and this might provide prolonged stimulatory signals to specific B cells and result in their terminal differentiation and functional exhaustion, as seen in other persistent infections (3–5). Such a scenario fits with the maturation defects of HBsAg-specific B cells present in patients with HBsAg positivity, but it is somehow surprising that we could not find any associations between HBsAg quantity and functional defects. For example, the ability of CD40L feeder cells to rescue HBsAg-specific B cell function was detected in CHB patients characterized by different clinical and virological profiles (HBsAg and HBV DNA quantity).

Similarly, the phenotype of HBsAg-specific B cells present in CHB patients only partially fits with their functional defects. An enrichment of HBsAg-specific B cells with a phenotype of atypi-

cal MBCs is clearly present in CHB patients (our data and Burton et al., ref. 50). These B cells were characterized by low CD21 and high CD69 and PD-1 expression, compatible with overstimulation and exhaustion. However, in all of the CHB patients studied here, such phenotypic features affect on average only approximately 15% of the HBsAg-specific B cells. Furthermore, HBsAg-specific B cells detected during acute hepatitis B are unable to expand and/or differentiate in vitro, but they did not display the phenotypic features detected in cells of CHB patients.

Analysis of gene expression at the single-cell level will be necessary to understand whether multiple mechanisms able to suppress the in vitro maturation of the different populations of HBsAg-specific B cells exist in vivo. At the moment, the technical challenge of sorting a sizeable number of HBsAg-specific B cells of different phenotypes (AtM, RM, and AM) precludes this analysis.

In addition, an in-depth analysis of HBV-specific T helper cells and especially Tfh cells, which provide help for B cell maturation via CD40L and IL-21 in the germinal center, in association with B cells will be important for better understanding the causes of HBsAg-specific B cell defects. Recent data in mouse models have shown the importance of boosting the T helper and Tfh cell responses for HBsAg seroconversion (51, 52), but data on Tfh cells in humans remain limited (53).

One other limitation of our analysis needs to be highlighted: the circulating compartment could not be the correct anatomical location for B cell quantity and functional analysis. The vast majority of B cells resides in the lymph nodes, where the process of IgG somatic maturation takes place (49). In addition, HBsAg-specific B cells can also be compartmentalized, not only in spleen and lymph nodes, but also in HBV chronic infected livers, as recently detected by Burton et al. (50). However, the finding that both circulating and intrahepatic B cells of CHB patients are enriched of atypical MBCs (50) demonstrates that the circulating compartment is representative of the global B cell features of HBV-infected patients.

We should also consider the fact that our method based on the use of recombinant HBsAg likely underestimated the real number of total HBsAg-specific B cells in HBV-infected patients. Abs recognize not only linear, but also conformational epitopes. The recombinant HBsAg used in our approach, although produced in mammalian cells (54), may have a different conformation than the natural envelope protein synthesized by infectious hepatocytes and present on the surface of the virions and of the defective HBsAg particles. In addition, circulating HBsAg could mask some HBsAg-specific B cells. Both issues make it likely that in HBV-infected patients, the absolute quantity of HBsAg-specific B cells is higher than what we can measure.

Perhaps this inability to visualize the totality of HBsAg-specific B cells might partially explain the other interesting finding of our work, the fact that global, non–HBV-specific B cell populations display a gene expression profile that was altered by HBV infection and share activation of genes involved in hyperstimulation and suppression of differentiation (*CD83*, *DUSP-4*) that support the B cell maturation defects of HBsAg-specific B cells. It will certainly be important to precisely measure the overall size of the HBV-specific B cell repertoire. This will allow understanding whether HBV infection alters the B cell compartment irrespective of their antigen specificity or whether the analysis with fluorochrome-conjugated HBsAg underestimates the HBV-specific B cell quantity. At the moment, our data indicate that both HBsAg-specific and total B cells are altered and that the total B cell alteration is more pronounced than what we detected on total T cells. This observation is in line with data showing that only a few total T cells express more exhaustion markers in CHB patients than in healthy individuals (55) and also with reports of preferential modifications of gene signatures of B cells induced by CHB infection (13, 36). The unanswered question is whether the modifications of both HBsAg-specific and total B cells are caused only by circulating HBsAg, other viral products, or by mechanisms not linked to virological products, such as an altered intrahepatic environment present in CHB patients, as suggested by Burton et al. (50). The full understanding of the contribution of these mechanisms on B cell functionality in CHB infection will be important for selecting the new therapeutic strategies that aim to recover the faulted HBV-specific immunity present in CHB patients and that are now entering clinical trials (23, 29, 56).

Agents designed to reduce secretion or synthesis of HBsAg might indeed restore HBV immune function, since, to our knowledge, our observation that full HBsAg-specific B cell functionality is recovered only at the time of complete negativity of serological HBsAg represents what we believe is the first clear observation that circulating HBsAg acts, in HBV-infected patients, not only as a decoy of anti-HBs Abs (28), but also as a modulator of HBsAg-specific B cell function. On the other hand, the lack of associations between HBsAg quantity and HBsAg-specific B cell defects might indicate that partial suppression of HBsAg quantity cannot be sufficient to recover B cell immunity.

In contrast, the findings that anti–PD-1 Abs augment HBsAg-specific B cell recovery in all CHB patients tested suggest that anti-PD1 therapy in CHB patients might be able to improve both HBV-specific T and B cell functionality. This hypothesis is supported not only by our in vitro data, but also by the report of the ability of anti–PD-1 treatment to recover B cell functionality in SIV–infected macaques (45). In line with the B cell profile of HIV-infected individuals, humoral immunity in SIV-persistent infection should share the functional, phenotypic, and transcriptomic alteration detected by us (and by the accompanying Burton et al. paper, ref. 50) in the HBsAg-specific and global B cell compartment of CHB patients. Thus, we believe that anti–PD-1 therapy might be able to indeed also act on the altered B cell compartment of CHB patients.

In conclusion, dual staining with fluorochrome-conjugated HBsAg allowed us to directly visualize HBsAg-specific B cells in different categories of HBV-infected and vaccinated subjects and decipher the impact that HBV has on humoral adaptive immunity. We observed that, while HBV infection status does not affect the frequency of circulating HBsAg-specific B cells, the functional state of global and HBsAg-specific B cells is robustly affected by HBsAg presence. The demonstration that the compromised HBsAg-specific B cells of CHB patients are amenable to functionally recovering after HBsAg clearance or through utilization of anti–PD-1 Abs opens new therapeutic possibilities for achieving HBV functional cure and calls for a precise monitoring of B cell function during future clinical trials with new agents designed to boost HBV-specific immunity.

Methods

Patients. The healthy (non–HBV infected) group comprised 18 subjects who completed a standard HBsAg vaccination (Engenirix B, 20 μg HBsAg protein, GSK) scheduled at least 5 years before entering the study, with the exception of a subject who performed a new boost HBV vaccination and 5 healthy non–HBV-vaccinated subjects (anti-HBs negative and anti-HBc negative). Furthermore, 21 subjects with a clinical history of resolved acute hepatitis (anti-HBc$^+$ and anti-HBs$^+$), 11 patients with acute hepatitis B (HBsAg$^+$, IgM anti-HBc$^+$, high ALT; longitudinal samples were obtained from 6 of them), and 96 treatment-naive patients with CHB infection (HBsAg$^+$) were included. Table 1 summarizes clinical and virological parameters. CHB patients were categorized into standard phases using the criteria outlined in the EASL 2017 clinical practice guidelines on the management of HBV infection (32). Thus, classification and denomination of CHB patients used in this work are as follows: (a) HBeAg$^+$ chronic infection (eAg$^+$CInf): normal ALT (< 40 IU/l), HBeAg$^+$ and high HBV DNA; (b) HBeAg$^+$ chronic hepatitis (eAg$^+$CHep): elevated ALT, HBeAg$^+$; (c) HBeAg$^-$ chronic hepatitis (eAg$^-$CHep): elevated ALT, anti-HBe$^+$; and (d) HBeAg$^-$ chronic infection (eAg$^-$CInf): normal ALT, anti-HBe$^+$, low HBV DNA (32).

Clinical and virological parameters. On recruitment to the study, anti-HBs titers (in vaccinated subjects) or viral serology and HBV DNA levels (in HBV-infected subjects) were tested. HBsAg, HBeAg, and anti-HBe levels were measured with a chemiluminescent microparticle immunoassay (chemiluminescent microparticle immunoassay [CMIA]; Abbott Architect, Abbott Diagnostics), and where available, HBV genotype was recorded. HBV DNA levels in serum were quantified by real-time PCR (COBAS AmpliPrep/COBAS TaqMan HBV test v2.0; Roche Molecular Diagnostics).

Production of fluorescently labeled HBsAg. Recombinant HBsAg (genotype A) was produced by Gilead Sciences as described (54). For labeling, purified recombinant HBsAg proteins were individually conjugated with DyLight 550 or DyLight 650 fluorochromes (Thermo Scientific) according to the manufacturer's protocol. Briefly, 5 mg HBsAg (1 mg/ml) was mixed with 50 μg of each dye and incubated at room temperature (RT) for 1 hour. The labeling was neutralized by adding 50 μl of 1 M Tris pH 7. Excess fluorochrome was removed by dialysis against PBS. Labeling efficiency was determined as described in the manufacturer's protocol (on average 7 dye molecules per HBsAg particle).

PBMC isolation and flow cytometry analysis of total and HBsAg-specific B cells. PBMCs were isolated from peripheral blood by density centrifugation using Ficoll-Hypaque Plus (GE Healthcare) and were then cryopreserved. Cells were thawed and then directly used for ex vivo flow cytometry. For staining experiments, first viability assay was performed by incubation of the cells for 10 minutes at RT with Live/Dead Fixable Blue Stain Reagent (L23105; Life Technologies). A panel of 15 mouse anti-human monoclonal Abs against CD3, CD10, CD19, CD21, CD23, CD24, CD27, CD38, CD39, CD69, CD73, CD95, HLA-DR, IgG, and PD-1 (details of Abs in Supplemental Table 1) in combination with HBsAg-D550 and HBsAg-D650 was used. After live/dead staining and washing steps, cells (~3 million) were incubated with a mixture containing optimum concentrations of the Abs together with the 2 labeled HBsAg reagents in Brilliant Stain Buffer (BD) for 30 minutes on ice (50 μl in V-bottom 96-well plate). Following incubation, cells were washed and fixed with 1% formaldehyde before acquisition on LSR-Fortessa flow cytometry (BD).

The optimum concentration of the labeled HBsAg for staining was defined by testing samples obtained from healthy vaccinated and unvaccinated donors. Different concentrations of the reagents were tested for binding to MBCs to select a concentration that had reasonable staining intensity on B cells with no binding to T cells and minimal background staining in unvaccinated subjects (Supplemental Figure 1). For the entire study, 1 μg of each reagent/50 μl staining mixture was chosen. Analysis of flow cytometry data was performed using FlowJo software, version 10 (BD), and the nonlinear dimensionality reduction technique UMAP (35). We downsampled the global MBCs to 10,000 cells per sample and used a logicle transformation with width of linearization (w) = 0.1, top of the scale data value (t) = 500000, total plot width in asymptotic decades (m) = 4.5, and additional negative range to be included in the display in asymptotic decades (a) = 0.

Cell sorting. Cell sorting was performed for 3 purposes: (a) transcriptional analysis of different subsets of total B cells and CD4$^+$ and CD8$^+$ T cells; (b) functional analysis of AtM compared with naive and classical MBCs; and (c) functional analysis of HBsAg-specific B cells.

For NanoString analysis on subsets of total B and T cells, PBMCs were thawed and directly stained (no enrichment) using the following mixture of Abs: (a) T cell staining: anti-CD3, anti-CD19, anti-CD4, anti-CD8, anti-CD197 (CCR7), and anti-CD45RA; and (b) B cell staining: anti-CD3, anti-CD10, anti-CD19, anti-CD21 and anti-CD27. For sorting of HBsAg-specific B cells, B cells were preenriched using EasySep human B Cell Isolation Kit (STEMCELL Technologies) to a purity of greater than 95%. Following live/dead staining, cells were stained with anti-CD3, anti-CD10, anti-CD19, anti-CD21, and anti-CD27 plus HBsAg-D550/650. An average of 300 HBsAg-specific B cells for the experiments without feeder cells and 150 specific cells for coculture with feeder cells were sorted. All sorts were performed with the FACSAria III machine (BD).

Functional analysis of HBsAg-specific B cells in vitro. All cultures were performed in Iscove's Modified Dulbecco's Medium (IMDM) (Invitrogen) and 10% ultra-low IgG fetal bovine serum (Gibco, Thermo Fisher Scientific) supplemented with 50 μg/ml human transferrin and 5 μg/ml human insulin (Sigma-Aldrich) (now called IMDM complete medium) in U-bottom 96-well culture plates. For functional characterization of HBsAg-specific B cells, cells were cultured in 2 different settings as follow: (a) sorted HBsAg-specific B cells from preenriched B cells of healthy vaccinated, acute, and chronic HBV–infected patients were cultured in vitro with optimized conditions for B cell expansion and differentiation to Ab-secreting cells reported by M. Jourdan (57) with few modifications. Briefly, sorted HBsAg-specific B cells from each subject were seeded in 100 μl/well IMDM complete medium containing 20 U/ml IL-2, 50 ng/ml IL-10, 10 ng/ml IL-15, 10 μg/ml phosphorothioate CpG oligodeoxynucleotide 2006 (ODN) (Invivogen), and 50 ng/ml monomeric soluble recombinant human CD40L (all cytokines and s-CD40L were purchased from R&D Systems). Cells were cultured 4 days under these conditions (step 1 to stimulate/expand B cells), then pelleted and resuspended in new medium containing 20 U/ml IL-2, 50 ng/ml IL-10, 10 ng/ml IL-15, and 50 ng/ml IL-6. Cells were cultured for another 3 days under these condition (step 2) to enhance their differentiation to Ab-producing plasmablasts. After 7 days of culture in these 2 steps, supernatants were collected and cells were washed and resuspended in fresh medium as in step 2 and seeded into ELISpot plates. (b) Sorted HBsAg-specific B cells were cocultured with irradiated 3T3-msCD40L feeder cells (3T3-mouse fibroblast cell line over-

expressing CD40L) (gift from Mark Connors, NIH/National Institute of Allergy and Infectious Diseases [NIAID], Bethesda, Maryland, USA) according to a protocol explained in detail previously (Huang et al., ref. 34). Briefly, irradiated 3T3-msCD40L cells were cultured in U-bottom 96-well plates to 70% confluency in DMEM medium containing 10% FBS. After 1 day, sorted HBsAg-specific B cells were resuspended in 200 μl IMDM complete medium containing IL-2 (200 U/ml) and IL-21 (50 ng/ml) and transferred to wells containing feeder cells. For PD-1 blockade experiments, 5 μg/ml anti–PD-1 (gift of Cheng-I Wang, Singapore Immunology Network, Singapore, ref. 58) was added into the culture medium during the entire experiment. After 13 days, cultured cells were washed and resuspended in fresh medium with IL-2, IL-21, and IL-6 (50 ng/ml) and then seeded into ELISpot plates.

Functional analysis of AtM compared with naive and classical MBCs in vitro. 2,000 Sorted total naive, RM, AM, and AtM B cells were cultured 7 days in 2 steps with CpG polyclonal stimulation, as described above. Cell-culture supernatants were collected after both steps and tested to measure total IgG concentration using the Human IgG Total ELISA kit (eBioscience) according to the manufacturer's instructions.

ELISpot assays. ELISpot assays for the detection of anti-HBs–producing cells were performed on expanded B cells based on a protocol by M. Jahnmatz et al. (59) with some modifications. Briefly, ELISpot plates (Millipore) were pretreated with 35% ethanol, washed, and coated with 1 μg/well (10 μg/ml) r-HBsAg (produced by Gilead Sciences; ref. 54) overnight at 4°C. Plates were washed and blocked; then, expanded B cells were added and incubated for 18 hours. IgG anti-HBs–secreting B cells were detected by the addition of biotin-conjugated goat Abs specific for human IgG-Fc (Mabtech, MT78/145), then ALP-conjugated streptavidin (BD), followed by development of plates using BCIP/NBT (Pierce, catalog 34034) and counting by the ImmunoSpot Image Analyzer 3.2 (Cellular Technology).

Anti-HBs ELISA. The MONOLISA anti-HBs Plus Kit (Bio-Rad) was used for measuring concentrations of anti-HBs Ab in the serum of the healthy vaccinated subjects as well as in culture supernatants of sorted specific B cells after expansion in vitro, based on the manufacturer's instructions.

NanoString gene expression analysis. Four different subsets of B cells and $CD4^+$ and $CD8^+$ T cell subsets obtained by cell sorting were lysed in RTL lysis buffer (QIAGEN, supplemented with 2-mercaptoethanol at 1:100) at a ratio of 1 μl RLT to 10,000 cells. Cell lysates from a minimum of 10,000 cells were analyzed using the preassembled nCounter GX Human Immunology Kit and the nCounter System (NanoString Technologies) according to the manufacturer's instructions. Data analysis and heatmap representation were performed with nSolver Analysis Software (version 3) provided by NanoString Technologies. Expression of 588 different genes was normalized based on the geometric means of both the supplied positive controls and the panel of 15 reference genes, as recommended by the manufacturer. Only genes that were significantly different ($P < 0.05$, *t* test, FDR adjusted) and at least 2-fold differentially expressed between the 2 groups of patients or 2 cell subsets were considered.

Statistics. Statistical analyses were performed in Prism (GraphPad) using the nonparametric 2-tailed Mann-Whitney *U* test, the nonparametric Kruskal-Wallis test followed by Dunn's multiple comparison test, Spearman's rank correlation, or Wilcoxon's paired *t* test as stated in the figure legends. $P \leq 0.05$ was considered significant.

Study approval. Blood donors were recruited from the viral hepatitis clinic at the Royal London Hospital and acute dengue samples from Tan Tock Seng Hospital in Singapore. Written informed consent was obtained from all subjects. The study was conducted in accordance with the Declaration of Helsinki and approved by the Barts and the London NHS Trust local ethics review board, the National Research Ethics Service Committee London–Research Ethics Committee (reference 10/H0715/39), and the Singapore National Healthcare Group ethical review board (DSRB 2008/00293).

Author contributions

LS performed experiments. LS, NLB, and AB designed experiments, analyzed and interpreted the data, and wrote the manuscript. CAD and EWN contributed to UMAP analysis. CF, MH, NN, and SF prepared and provided materials. USG performed some experiments and, with PTFK, recruited patients, performed clinical monitoring, and provided clinical expertise. All authors provided critical review and approved the manuscript.

Acknowledgments

We thank all patients, their families, and control volunteers who participated in this study. We would like to thank Mark Connors (NIH) for providing the 3T3-msCD40L cell line, Cheng-I Wang (Singapore Immunology Network) for the anti–PD-1 Ab, Laura Rivino (Duke-NUS), and Yee Sin Leo (Tan Tock Seng Hospital) for providing acute dengue patient samples, and also Charlene Foong Shu Fen at the SingHealth Flow Cytometry Core Facility for help on sorting experiments. This work was supported by a Singapore Translational Research (STaR) investigator award (NMRC/STaR/013/2012 to AB) and by the Eradication of HBV TCR Program (NMRC/TCR/014-NUHS/2015 to AB and EWN), a Wellcome Trust Clinical Research Training Fellowship (107389/Z/15/Z to USG), and a Barts and The London Charity Large Project grant (723/1795 to PTFK).

Address correspondence to: Antonio Bertoletti, Emerging Infectious Diseases Program, DUKE-NUS Medical School, 8 College Road, Singapore 169857. Phone: 65.6601.3574; Email: antonio@duke-nus.edu.sg.

1. Oxenius A, Zinkernagel RM, Hengartner H. Comparison of activation versus induction of unresponsiveness of virus-specific $CD4^+$ and CD8+ T cells upon acute versus persistent viral infection. *Immunity*. 1998;9(4):449–457.
2. Wherry EJ, et al. Molecular signature of $CD8^+$ T cell exhaustion during chronic viral infection. *Immunity*. 2007;27(4):670–684.
3. Moir S, et al. Evidence for HIV-associated B cell exhaustion in a dysfunctional memory B cell compartment in HIV-infected viremic individuals. *J Exp Med*. 2008;205(8):1797–1805.
4. Portugal S, et al. Malaria-associated atypical memory B cells exhibit markedly reduced B cell receptor signaling and effector function. *Elife*. 2015;4:e07218.
5. Sullivan RT, et al. FCRL5 delineates functionally impaired memory B cells associated with Plasmodium falciparum exposure. *PLoS Pathog*. 2015;11(5):e1004894.
6. Bertoletti A, Ferrari C. Adaptive immunity in HBV infection. *J Hepatol*. 2016;64(1 suppl):S71–S83.
7. Maini MK, et al. The role of virus-specific CD8(+) cells in liver damage and viral control during persistent hepatitis B virus infection. *J Exp Med*. 2000;191(8):1269–1280.
8. Boni C, et al. Characterization of hepatitis B virus (HBV)-specific T-cell dysfunction in chronic HBV infection. *J Virol*. 2007;81(8):4215–4225.
9. Kurktschiev PD, et al. Dysfunctional $CD8^+$ T cells

in hepatitis B and C are characterized by a lack of antigen-specific T-bet induction. *J Exp Med*. 2014;211(10):2047–2059.
10. Bengsch B, Martin B, Thimme R. Restoration of HBV-specific CD8+ T cell function by PD-1 blockade in inactive carrier patients is linked to T cell differentiation. *J Hepatol*. 2014;61(6):1212–1219.
11. Schurich A, et al. Distinct metabolic requirements of exhausted and functional virus-specific CD8 T cells in the same host. *Cell Rep*. 2016;16(5):1243–1252.
12. Fisicaro P, et al. Targeting mitochondrial dysfunction can restore antiviral activity of exhausted HBV-specific CD8 T cells in chronic hepatitis B. *Nat Med*. 2017;23(3):327–336.
13. Oliviero B, et al. Enhanced B-cell differentiation and reduced proliferative capacity in chronic hepatitis C and chronic hepatitis B virus infections. *J Hepatol*. 2011;55(1):53–60.
14. Xu X, et al. Reversal of B-cell hyperactivation and functional impairment is associated with HBsAg seroconversion in chronic hepatitis B patients. *Cell Mol Immunol*. 2015;12(3):309–316.
15. Dusheiko GM, Hoofnagle JH, Cooksley WG, James SP, Jones EA. Synthesis of antibodies to hepatitis B virus by cultured lymphocytes from chronic hepatitis B surface antigen carriers. *J Clin Invest*. 1983;71(5):1104–1113.
16. Barnaba V, et al. Immunoregulation of the in vitro anti-HBs antibody synthesis in chronic HBsAg carriers and in recently boosted anti-hepatitis B vaccine recipients. *Clin Exp Immunol*. 1985;60(2):259–266.
17. Böcher WO, et al. Regulation of the neutralizing anti-hepatitis B surface (HBs) antibody response in vitro in HBs vaccine recipients and patients with acute or chronic hepatitis B virus (HBV) infection. *Clin Exp Immunol*. 1996;105(1):52–58.
18. Barnaba V, Franco A, Alberti A, Benvenuto R, Balsano F. Selective killing of hepatitis B envelope antigen-specific B cells by class I-restricted, exogenous antigen-specific T lymphocytes. *Nature*. 1990;345(6272):258–260.
19. Maruyama T, et al. Distinguishing between acute and symptomatic chronic hepatitis B virus infection. *Gastroenterology*. 1994;106(4):1006–1015.
20. Tian C, et al. Use of ELISpot assay to study HBs-specific B cell responses in vaccinated and HBV infected humans. *Emerg Microbes Infect*. 2018;7(1):16.
21. Gerlich WH. The enigma of concurrent hepatitis B surface antigen (HBsAg) and antibodies to HBsAg. *Clin Infect Dis*. 2007;44(9):1170–1172.
22. Zoulim F, Lebossé F, Levrero M. Current treatments for chronic hepatitis B virus infections. *Curr Opin Virol*. 2016;18:109–116.
23. Gish RG, et al. Chronic hepatitis B: Virology, natural history, current management and a glimpse at future opportunities. *Antiviral Res*. 2015;121:47–58.
24. Bruss V. Hepatitis B virus morphogenesis. *World J Gastroenterol*. 2007;13(1):65–73.
25. Urban S, Bartenschlager R, Kubitz R, Zoulim F. Strategies to inhibit entry of HBV and HDV into hepatocytes. *Gastroenterology*. 2014;147(1):48–64.
26. Schilling R, et al. Endocytosis of hepatitis B immune globulin into hepatocytes inhibits the secretion of hepatitis B virus surface antigen and virions. *J Virol*. 2003;77(16):8882–8892.
27. Zhang TY, et al. Prolonged suppression of HBV in mice by a novel antibody that targets a unique epitope on hepatitis B surface antigen. *Gut*. 2016;65(4):658–671.
28. Rydell GE, Prakash K, Norder H, Lindh M. Hepatitis B surface antigen on subviral particles reduces the neutralizing effect of anti-HBs antibodies on hepatitis B viral particles in vitro. *Virology*. 2017;509:67–70.
29. Lindh M, Rydell GE, Larsson SB. Impact of integrated viral DNA on the goal to clear hepatitis B surface antigen with different therapeutic strategies. *Curr Opin Virol*. 2018;30:24–31.
30. Ward SM, Phalora P, Bradshaw D, Leyendeckers H, Klenerman P. Direct ex vivo evaluation of long-lived protective antiviral memory B cell responses against hepatitis B virus. *J Infect Dis*. 2008;198(6):813–817.
31. Townsend SE, Goodnow CC, Cornall RJ. Single epitope multiple staining to detect ultralow frequency B cells. *J Immunol Methods*. 2001;249(1–2):137–146.
32. European Association for the Study of the Liver. EASL 2017 clinical practice guidelines on the management of hepatitis B virus infection. *J Hepatol*. 2017;67(2):370–398.
33. Webster GJ, et al. Longitudinal analysis of CD8$^+$ T cells specific for structural and nonstructural hepatitis B virus proteins in patients with chronic hepatitis B: implications for immunotherapy. *J Virol*. 2004;78(11):5707–5719.
34. Huang J, et al. Isolation of human monoclonal antibodies from peripheral blood B cells. *Nat Protoc*. 2013;8(10):1907–1915.
35. Becht E, Dutertre CA, Kwok IWH, Ng LG, Ginhoux F, Newell EW. Evaluation of UMAP as an alternative to t-SNE for single-cell data. *bioRxiv*. CSH website. https://www.biorxiv.org/content/early/2018/04/10/298430. doi: https://doi.org/10.1101/298430. Published April 10, 2018. Accessed August 16, 2018.
36. Vanwolleghem T, et al. Re-evaluation of hepatitis B virus clinical phases by systems biology identifies unappreciated roles for the innate immune response and B cells. *Hepatology*. 2015;62(1):87–100.
37. Kardava L, et al. Abnormal B cell memory subsets dominate HIV-specific responses in infected individuals. *J Clin Invest*. 2014;124(7):3252–3262.
38. Obeng-Adjei N, et al. Malaria-induced interferon-γ drives the expansion of Tbethi atypical memory B cells. *PLoS Pathog*. 2017;13(9):e1006576.
39. Knox JJ, Kaplan DE, Betts MR. T-bet-expressing B cells during HIV and HCV infections. *Cell Immunol*. 2017;321:26–34.
40. Kretschmer B, et al. CD83 modulates B cell function in vitro: increased IL-10 and reduced Ig secretion by CD83Tg B cells. *PLoS One*. 2007;2(8):e755.
41. Hanihara F, Takahashi Y, Okuma A, Ohba T, Muta T. Transcriptional and post-transcriptional regulation of IκB-ζ upon engagement of the BCR, TLRs and FcγR. *Int Immunol*. 2013;25(9):531–544.
42. Yu M, et al. Signal inhibition by the dual-specific phosphatase 4 impairs T cell-dependent B-cell responses with age. *Proc Natl Acad Sci U S A*. 2012;109(15):E879–E888.
43. Thibult ML, et al. PD-1 is a novel regulator of human B-cell activation. *Int Immunol*. 2013;25(2):129–137.
44. Kardava L, et al. Attenuation of HIV-associated human B cell exhaustion by siRNA downregulation of inhibitory receptors. *J Clin Invest*. 2011;121(7):2614–2624.
45. Velu V, et al. Enhancing SIV-specific immunity in vivo by PD-1 blockade. *Nature*. 2009;458(7235):206–210.
46. Maini MK, et al. Direct ex vivo analysis of hepatitis B virus-specific CD8(+) T cells associated with the control of infection. *Gastroenterology*. 1999;117(6):1386–1396.
47. Lee J, et al. Rituximab and hepatitis B reactivation in HBsAg-negative/ anti-HBc-positive kidney transplant recipients. *Nephrol Dial Transplant*. 2017;32(4):722–729.
48. Paul S, et al. Role of surface antibody in hepatitis B reactivation in patients with resolved infection and hematologic malignancy: A meta-analysis. *Hepatology*. 2017;66(2):379–388.
49. Kuka M, Iannacone M. Viral subversion of B cell responses within secondary lymphoid organs. *Nat Rev Immunol*. 2018;18(4):255–265.
50. Burton AR, et al. Circulating and intrahepatic antiviral B cells are defective in hepatitis B. *J Clin Invest*. 2018;128(10):4588–4603.
51. Publicover J, et al. An OX40/OX40L interaction directs successful immunity to hepatitis B virus. *Sci Transl Med*. 2018;10(433):eaah5766.
52. Wang X, et al. Dysregulated response of follicular helper T cells to hepatitis B surface antigen promotes HBV persistence in mice and associates with outcomes of patients. *Gastroenterology*. 2018;154(8):2222–2236.
53. Li Y, et al. Circulating chemokine (C-X-C Motif) receptor 5(+) CD4(+) T cells benefit hepatitis B e antigen seroconversion through IL-21 in patients with chronic hepatitis B virus infection. *Hepatology*. 2013;58(4):1277–1286.
54. Tharinger H, et al. Antibody-dependent and antibody-independent uptake of HBsAg across human leucocyte subsets is similar between individuals with chronic hepatitis B virus infection and healthy donors. *J Viral Hepat*. 2017;24(6):506–513.
55. Kennedy PTF, et al. Preserved T-cell function in children and young adults with immune-tolerant chronic hepatitis B. *Gastroenterology*. 2012;143(3):637–645.
56. Seeger C. Control of viral transcripts as a concept for future HBV therapies. *Curr Opin Virol*. 2018;30:18–23.
57. Jourdan M, et al. An in vitro model of differentiation of memory B cells into plasmablasts and plasma cells including detailed phenotypic and molecular characterization. *Blood*. 2009;114(25):5173–5181.
58. Na Z, et al. Structural basis for blocking PD-1-mediated immune suppression by therapeutic antibody pembrolizumab. *Cell Res*. 2017;27(1):147–150.
59. Jahnmatz M, Kesa G, Netterlid E, Buisman AM, Thorstensson R, Ahlborg N. Optimization of a human IgG B-cell ELISpot assay for the analysis of vaccine-induced B-cell responses. *J Immunol Methods*. 2013;391(1–2):50–59.